PSYCHOLOGY AND EDUCATION (2021) 58(4): 2406-2416
Article Received: 08th October, 2020; Article Revised: 15th February, 2021; Article Accepted: 20th March, 2021

Exploring the Correlation between Land Surface Temperature, NDBI, NDVI, and NDMI over Gombe Metropolis, Nigeria

Abdulkadir I[1], SathishKumar[2]
[1] Geography Unit, School of Basic and Remedial Studies, Gombe State University, Gombe, Gombe State, Nigeria
[2] Department of Civil Engineering, SRM institute Science and Technology, Chennai, India
Email: [1] abdish@ymail.com, [2] sathishj1@srmist.edu.in

ABSTRACT

Condition of being urbanized involves the substitution of natural environment with man-made surfaces built from imperviable materials, and such reduce vegetation cover result in the absorption of sun's energy, causing skin temperatures of the Earth and the temperatures of the air near surface to rise. It is on this note that this paper set out to assess the correlation between Land Surface Temperature (LST), and Normalized Difference Built-Up Index (NDBI), Normalized Difference Vegetation Index (NDVI), Normalized Difference Moisture Index (NDMI) over Gombe Metropolis at three different periods (January, 30th, May 22nd and September 30th, 2019) using Landsat 8 in ArcGIS. The result shows that there is a strong positive relationship between LST and NDBI in the three periods of studies with R^2 = 0.9935 (January 30th), 0.9863 (May 22nd) and 0.9923 (September 30th). The result also indicated a strong negative relation between LST and NDVI in the three periods with R^2 = 0.5922 (January 30th), 0.7487 (May 22nd) and 0.6017 (September 30th). The LST and NDMI correlation also shows a negative relationship with R^2= 0.5399 (January 30th), 0.7115 (May 22nd) and 0.568 (September 30th).

Keywords

Land Surface Temperature, NDBI, NDVI, NDMI and Landsat 8

Introduction

Land uptake for urbanization involves the process of replacement of the natural environment with a cultural one, mostly built from impervious materials [1], thereby affecting the radiative and thermal properties of the environment. These imperviable surfaces absorb greater percentage of the sun's energy than reflecting it, causing surface temperatures and air temperatures to rise due to their thermal storage capacity. In this paper, Land Surface Temperature (LST) can be defined as the temperature of the thin layer of the Earth surface that interacts with the mechanical mixture of gases near the surface.

Scholars have elucidated on the relevance of LST from urban studies to trends assessment pertaining hydrological cycle, climate variability, evapotranspiration and urban climate [2]–[9], monitoring and prediction of crop output [10], and modeling of vegetal stress [11]–[14]. LST can be observed using data obtained from the terrestrial platform, but satellite thermal infrared (TIR) data (Landsat 4, 5, 7 & 8, and Moderate Resolution Imaging Spectroradiameter (MODIS) Terra & Aqua, Advance Space Borne Thermal Emission and Reflection Radiometer (ASTER) Sentinel 2A & 2B, Sentinel 3A & 3B etc.), is the most widely used in assessing LST [15]–[22].

The urbanized areas and public places become congested of some kind for daily human and economic activities [23], air condition, transportation, and other bake businesses release heat that contribute to the rising temperature during daytime [24]–[26] thereby increasing and leaving behind the footprint of heat island though there is a drastic fall at night due to reduction of activities [27]. Therefore built-up areas and bare surface experience an increase in surface and near-surface temperature [28]–[31]. Notwithstanding some studies reported the opposite pointing that the built-up areas (arid/semi-arid regions) experience a lessening surface temperature [32]–[33], they show an attribute of wetness as the sole deciding factor of the surface temperature [34] where the surrounding dry and bare soil have higher surface temperature than the built-up/sealed areas.

Monitoring spatiotemporal variations of LST and its correlation between normalized difference vegetation index (NDVI), normalized difference built-up index (NDBI), normalized difference moisture index (NDMI), leaf area index (LAI) etc. using linear regression technique, has been one of the point of research in recent time [35]–[46]. In

Article Received: 08th October, 2020; Article Revised: 15th February, 2021; Article Accepted: 20th March, 2021

the foregoing, part of the outcome of the correlation analysis especially pertaining LST and NDVI among the scholars was not consistent, the results range from negative correlation [17], [42]–[43], [47] to relatively positive correlation [48] to no correlation [49].

Materials And Method

A. Materials

Landsat 8 datasets (January 30, May 22, and September 30, 2019) was used in ArcGIS for correlation of LST, NDBI, NDVI, and NDMI.

a) Computation land surface temperature using thermal bands (band 10 & 11).

i. Conversion of satellite DN to spectral radiance [50] for band 10 was computed using equation (1),

$$L_\lambda = M_L Q_{cal} + A_L \quad (1)$$

Where M_L is band specific multiplicative rescale factor,

Q_{cal} is quantized and calibrated standard product pixel value (DN)

A_L is band specific additive rescale factor.

ii. Conversion of spectral radiance to brightness temperature [50] using equation (2),

$$BT = \frac{K_2}{Ln\,(K_1/L_\lambda + 1)} - 273.15 \quad (2)$$

Where BT Brightness Temperature is at Satellite Brightness Temperature SBT,

K_1 & K_2 are thermal constant factors for either band 10 or 11

L_λ is radiance,

Ln is natural log,

– 273.15 is added to convert the temperature to degree Celsius.

iii. Computation of LST using equation (3),

$$LST = BT/1 + \lambda\,(BT/\rho)\ln(LSE) \quad (3)$$

Where BT is at Satellite Brightness Temperature

λ is the wavelength,

ρ is 14380,

LSE is land surface emissivity.

iv. Computation of land surface emissivity using equation (4),

$$LSE = 0.004P_V + 0.986 \quad (4)$$

Where P_V is Proportion of vegetation

v. Computation of proportional vegetation (Pv) using the equation (5), we derived P_V from NDVI

$$P_V = (NDVI – NDVI_{min}/NDVI_{max} - DVI_{min})^2 \quad (5)$$

Where, NDVI is Normalized Difference Vegetation Index.

vi. Computation normalized differential index NDVI using equation (6),

NDVI is the proportion of changes between near infrared and red bands to the sum of near infrared and red bands. It is used to assess above ground biomass health, determine vegetative or none vegetative areas.

$$NDVI = NIR – Red / NIR + Red \quad (6)$$

Where

NIR is near infrared is band 5 (Landsat 8),

Red is band 4 (Landsat 8).

The above procedures were repeated for band 11 and then average was computed between the two bands to obtain the LST.

b) Other indices for correlation analysis:

i Normalized Difference Built-Up Index (NDBI), was developed [51] to assess built-up areas. Computation of NDBI using equation (7),

$$NDBI = \frac{SWIR - NIR}{SWIR + NIR} \quad (7)$$

Where SWIR is band 6 (Landsat 8),

NIR is band 5 (Landsat 8).

ii Normalized Difference Moisture Index (NDMI), it highlights vegetation moisture of an area using the equation (8)

$$NDMI = \frac{NIR - SWIR}{NIR + SWIR} \quad (8)$$

Where NIR is band 5 (Landsat 8),

SWIR is band 6 (Landsat 8).

Correlation between LST and NDVI, NDBI, NDMI was computed using excel sheet.

B. Study Area

Gombe metropolis is the capital city of Gombe state, situated in the North Eastern part of Nigeria. It was named state capital when Gombe state was created from the then Bauchi state on 1st October, 1996. Gombe metropolis overlaps into Akko, Kwami and Yamaltu-Deba local government areas [52]. It has a projected population of about 400,000 in 2010 [53]. Fig.1 show Landsat satellite scene of the study area in near infrared, red and green. The urban areas can be seen in light-medium or dark blue colors, undeveloped surfaces in light brown-yellow, vegetation in red, roads in black, and geological outcrop in brown. Previous research reported that due to the reflection of the roofs of corrugated iron sheets, most African

PSYCHOLOGY AND EDUCATION (2021) 58(4): 2406-2416
Article Received: 08th October, 2020; Article Revised: 15th February, 2021; Article Accepted: 20th March, 2021

towns seen from space, appear in blue luminosity. The spectral attributes of these metal roofs differ with age, which is an important peculiarity allowing the differentiation of the urban structure and the monitoring of its development [54].

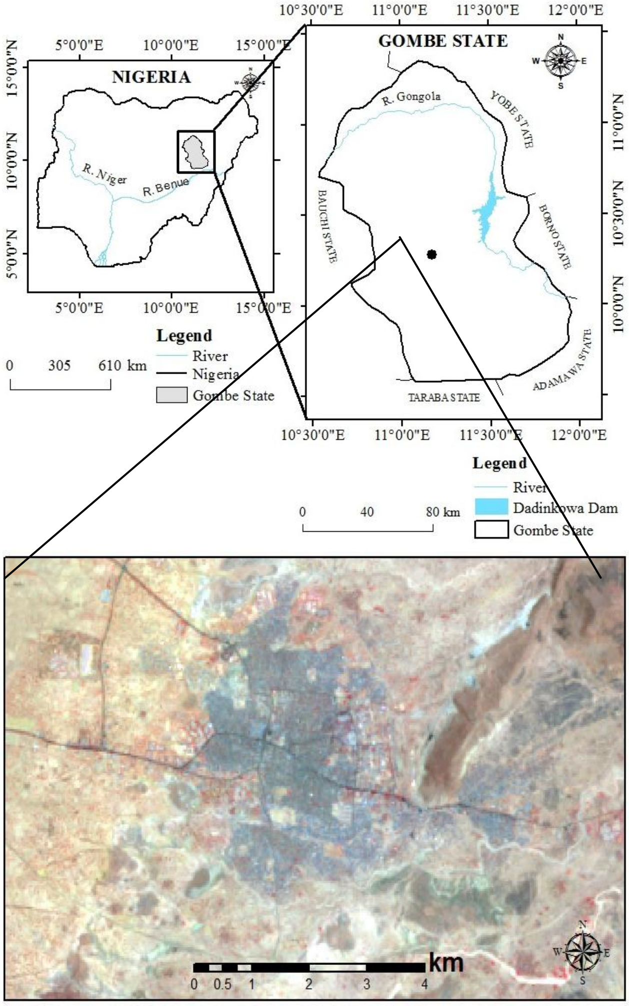

Source: Landsat, scene ID: 186-053; on 07-04-2000.

Fig. 1 Satellite image of Gombe Metropolis

Result and Discussion

A. Land Surface Temperature

Fig. 2 present spatial distribution of LST over Gombe metropolis and shows that landuse/landcover and season influence the land surface temperature statistics in table 1.

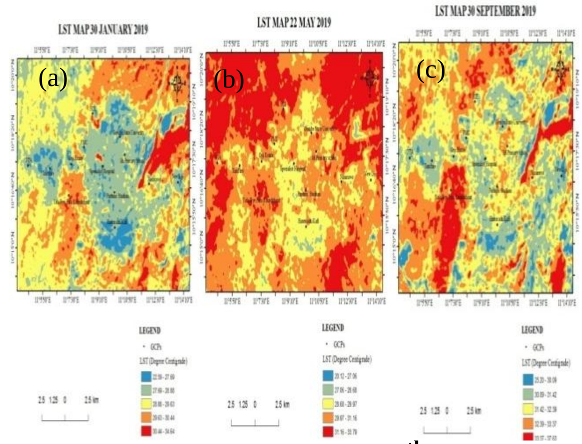

Fig. 2 LST Maps (a) January 30th LST map, (b) May 22nd LST map, (c) September 30th LST map.

Table 1 Mean LST Statistics

Date	Min (^{0}C)	Max (^{0}C)	Mean (^{0}C)	SD
30/1/19	22.59	34.64	29.59	0.9197
22/5/19	26.44	33.95	31.27	0.9326
30/9/19	25.20	37.68	32.21	1.1348

January 30th, LST maps recorded mean temperature of 29.59^{0}C and marked the lowest among three periods of this study. During this month (January), harmattan comes with dust/haze when visibility is poor, that absorbs, scatter and reflect the incoming sun's energy from reaching the earth's surface, therefore result into lower surface temperature. May 22nd, and September 30th LST maps recorded higher mean temperature of 31.27^{0}C and 32.21^{0}C respectively, during these months (May and September) the sky is clear and free from haze therefore, the sun's energy reaches the earth's surface causing the earth's thin layer and the mechanical mixture of gases near the surface to heat up more easily and result into higher surface temperature. The landcover of the study area is influence by number of landuse (residential, commercial, educational etc.) that gives rise to impervious/sealed surfaces, affecting number of ecosystem services.

It was observed that the built-up areas of the metropolis experience lower and graduated surface temperature in all the periods of this study than the surrounding rocks and bare surfaces. The above findings are consistent with the previous

PSYCHOLOGY AND EDUCATION (2021) 58(4): 2406-2416
Article Received: 08th October, 2020; Article Revised: 15th February, 2021; Article Accepted: 20th March, 2021

studies reported that the built-up areas (arid/semi-arid regions) experienced a lessening surface temperature [32]–[33], they show an attribute of wetness as the sole deciding factor of the surface temperature [34].

The maximum temperatures observed in all the three periods of this study were found on the surrounding rocks and bare surfaces.

B. Normalized Difference Vegetation Index

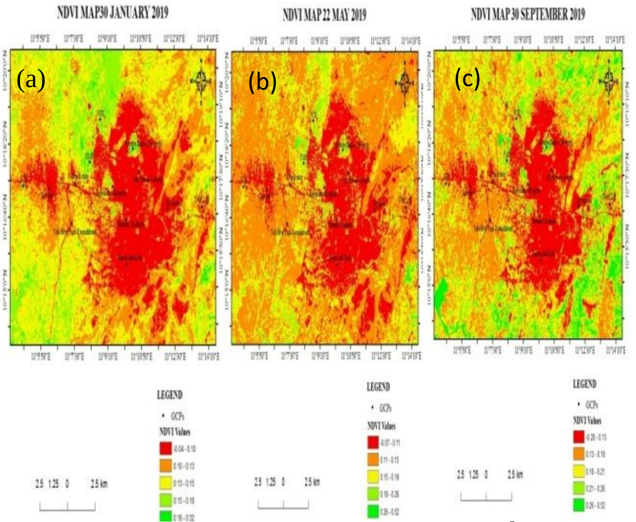

Fig. 3 NDVI Maps, (a) January 30th NDVI map, (b) May 22nd NDVI map, (c) September 30th NDVI map

Table 2 NDVI Statistics

Date	Min (^{0}C)	Max (^{0}C)	Mean (^{0}C)	SD
30/1/19	-0.0400	0.3198	0.1391	0.0221
22/5/19	-0.0717	0.5214	0.1505	0.0345
30/9/19	-0.28.34	0.5225	0.2062	0.0422

Fig. 3 present NDVI Maps and marked as a pointer that Landuse/Landcover and wet and dry seasons influence the NDVI statistics of Gombe metropolis (see table 2). The Land use/Landcover of the metropolis reveals that greater percentage of surface area is being sealed up from the atmosphere therefore recorded low NDVI values in all the three periods of study. The minimum NDVI value (-0.0717) among the three periods of this study was recorded on May 22nd, the NDVI map show significance of low values because of dry season, the vegetation also show sign of stress because of the insufficient soil moisture and low water table. The vegetated areas in the metropolis are part of Gombe State University, Federal Medical Center, Federal College of Education, and some selected areas outside the metropolis recorded higher NDVI values in all the three periods of study. The highest NDVI value of 0.5225 was recorded in the September 30, NDVI map.

C. LST and NDVI Correlation

Fig. 4 reveals a strong negative correlation between LST and NDVI in three periods of study with R^2 = 0.5922 (January 30th), 0.7487 (May 22nd) and 0.6017 (30th September). The negative correlation observed between LST and NDVI shows that NDVI does not induce surface temperature but rather vegetation cover provide natural cooling effects from shading and evapotranspiration whereas built-up areas, rocks and bare surfaces absorb sun's energy thereby causing the surface and air temperature to rise. It was observed variation in NDVI due to season influence surface temperature. This finding matches the result reported by [17], [42]–[43], [47] that there is a negative relationship between NDVI and LST

Article Received: 08th October, 2020; Article Revised: 15th February, 2021; Article Accepted: 20th March, 2021

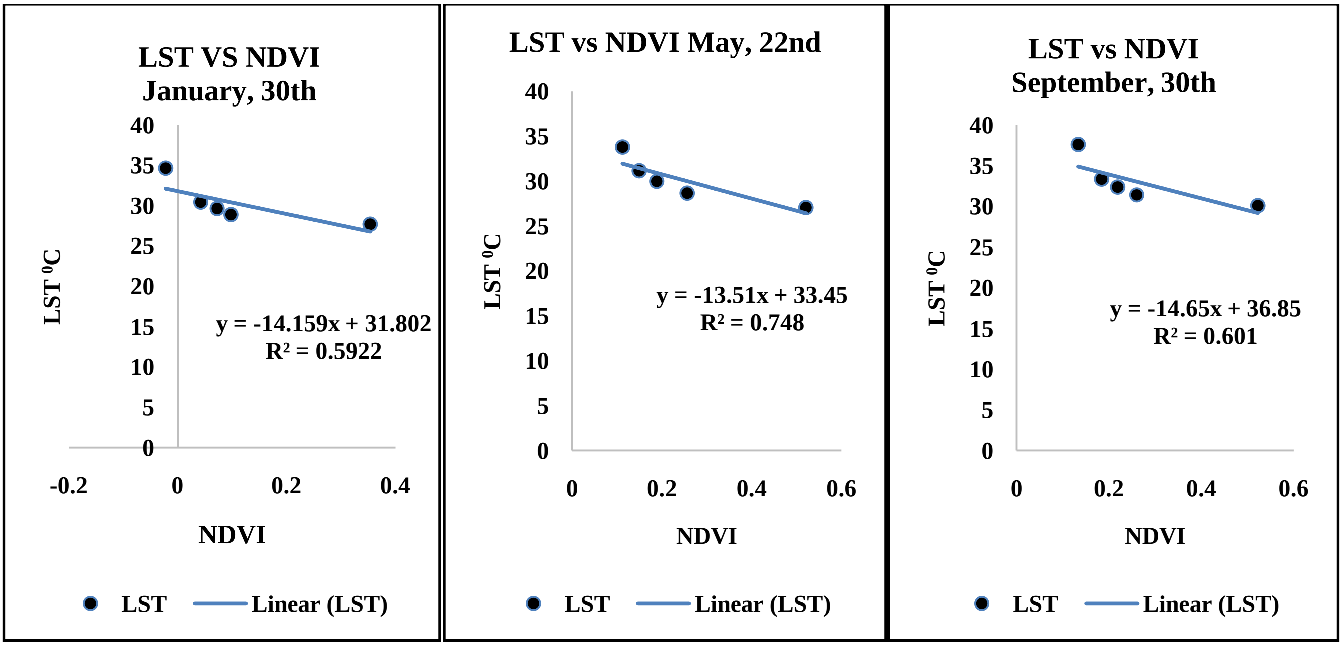

Fig. 4 Correlations between LST and NDVI

D. Normalized Difference Built-up Index

Table 3 shows NDBI statistics, the minimum values for the three periods are -0.2344, -0.3457, -0.3466 respectively. The maximum values 0.3539, 0.2561 and 0.3050 respectively. Mean NDBI are 0.0832, 0.0936 and 0.0341 respectively.

The result shows that the higher NDBI values are concentrated on rocks surfaces (Fig.5) in all the three periods of study. The results also indicate that the lower values were concentrated in vegetated areas in all the three periods of study.

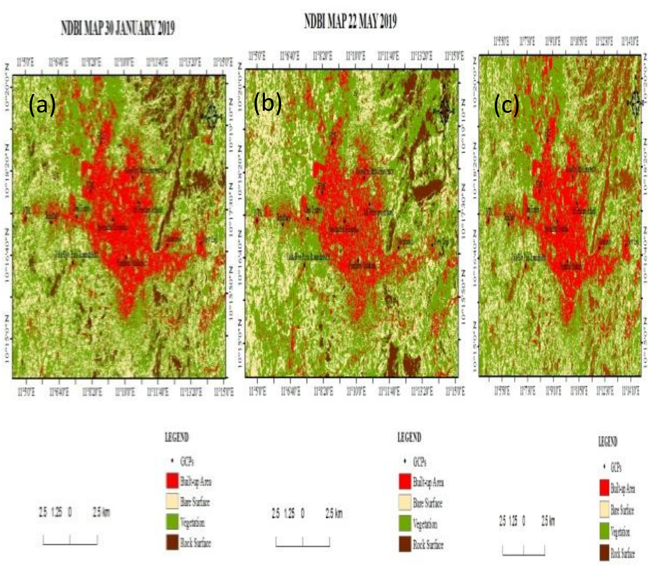

Fig. 5 NDVI Maps, (a) January 30th NDBI map, (b) May 22nd NDBI map, (c) September 30th NDBI map

Table 3 NDBI Statistics

Date	Min (⁰C)	Max (⁰C)	Mean (⁰C)	SD
30/1/19	-0.2324	0.3539	0.0832	0.0285
22/5/19	-0.3457	0.2561	0.0936	0.0368
30/9/19	-0.3466	0.3050	0.0341	0.0436

E. LST and NDBI Correction

Fig. 6 present a strong positive correlation between LST and NDBI in all the three periods with R^2 = 0.9935 (January 30th), 0.9863 (May 22nd) and 0.9923 (September 30th). Built-up/sealed surface understate the effect of vegetation and transpiration. This finding is consistent with previous study reported that there is positive relationship between LST and NDBI [43]. It was also reported that LST and NDBI relationship reveals that built-up areas produce LST based upon the behavior of the Earth's cover variation and result in UHI [43].

Article Received: 08th October, 2020; Article Revised: 15th February, 2021; Article Accepted: 20th March, 2021

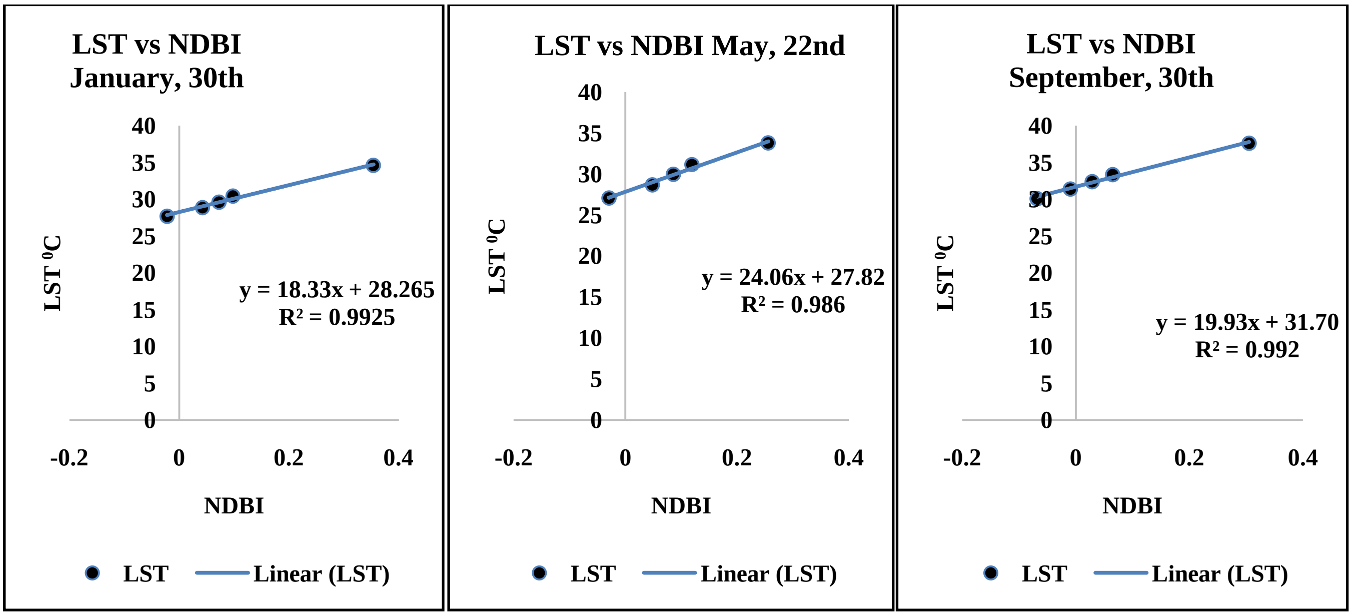

Fig. 6 Correlations between LST and NDBI

F. NDBI and NDVI Correlation

NDBI and NDVI correlation analysis in Fig. 7 shows a strong negative relationship in all the three periods of study with the R^2 = 0.5466, 0.7175, 0.5368 respectively. This finding matches a previous study reported that there is negative correlation between NDBI and NDVI [43]. NDVI is applied to describe stages of development and expansion of built-up area [17].

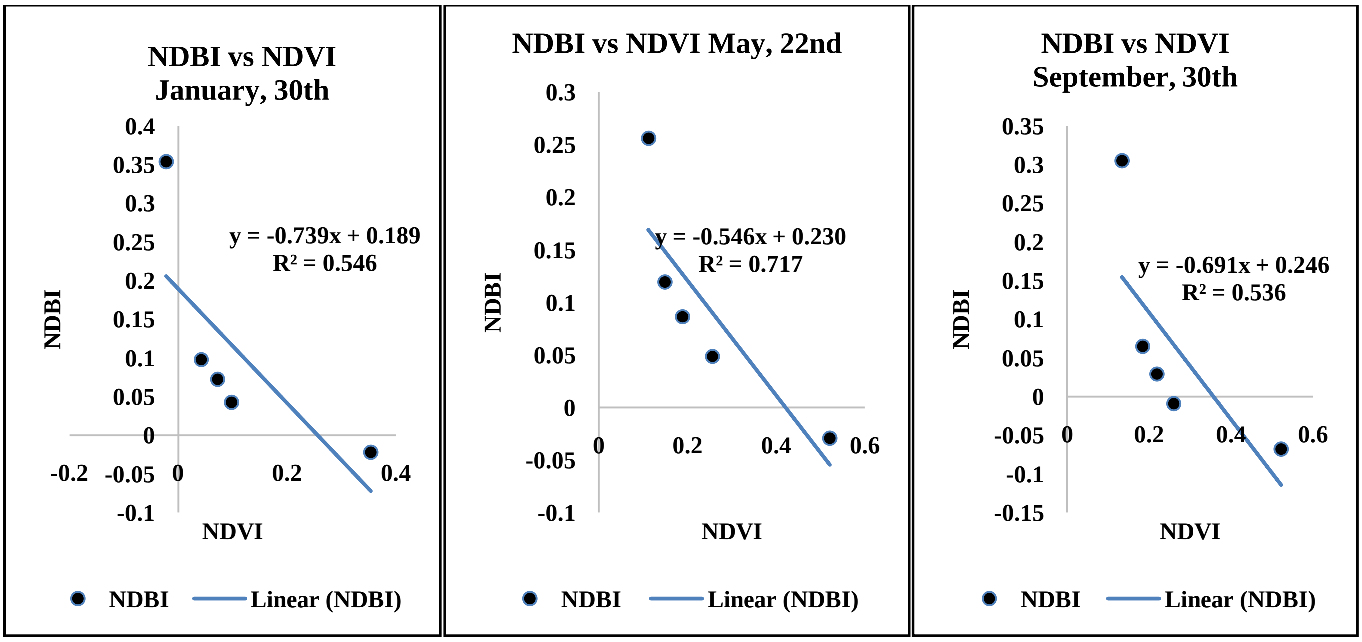

Fig. 7 Correlations between NDBI and NDVI

Article Received: 08th October, 2020; Article Revised: 15th February, 2021; Article Accepted: 20th March, 2021

G. Normalized Difference Moisture Index

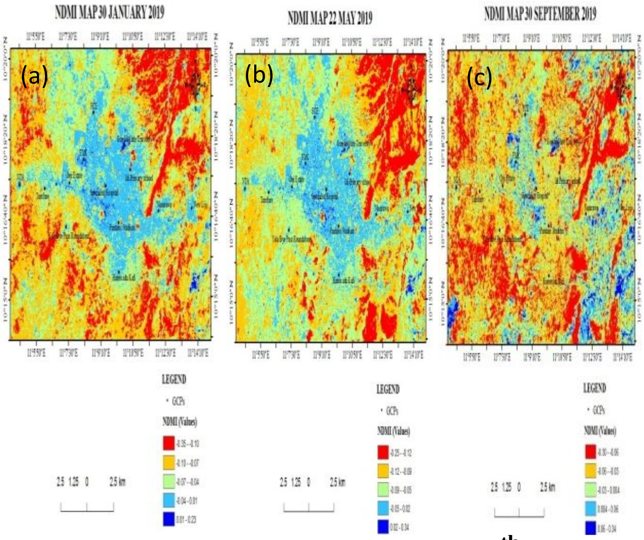

Fig. 8 NDMI Maps (a) January 30th NDMI map, (b) May 22nd NDMI map, (c) September 30th NDMI map

Table 4 NDMI Statistics

Date	Min (^{0}C)	Max (^{0}C)	Mean (^{0}C)	SD
30/1/19	-0.3539	0.2344	-0.0832	0.0285
22/5/19	-0.2561	0.3457	-0.0936	0.0368
30/9/19	-0.3050	0.3466	-0.0341	0.0436

Landuse/landcover, wet and dry seasons influence the NDMI Statistics in table 4. The result indicated that lowest values of -0.3539 was observed during January 30th NDMI and was found on rocks and bare surfaces. The maximum NDMI value of 0.3466 was observed during September 30th and was associated with vegetation cover in Gombe State University, Federal Medical Center, Federal College of Education, and other vegetated areas outside the squares of Gombe metropolis.

H. LST and NDMI Correlation

The outcome of the correlation analysis between LST and NDMI in Fig. 9 reveals a negative relationship with R^2= 0.5399 (January 30th), 0.7115 (May 22nd) and 0.5680 (September 30th). NDMI influence LST, areas with vegetation moisture in abundance are inclined to have relatively low LST values, when compared to built-up areas, rocks and bare surfaces with less vegetation moisture tend to have a relatively higher LST.

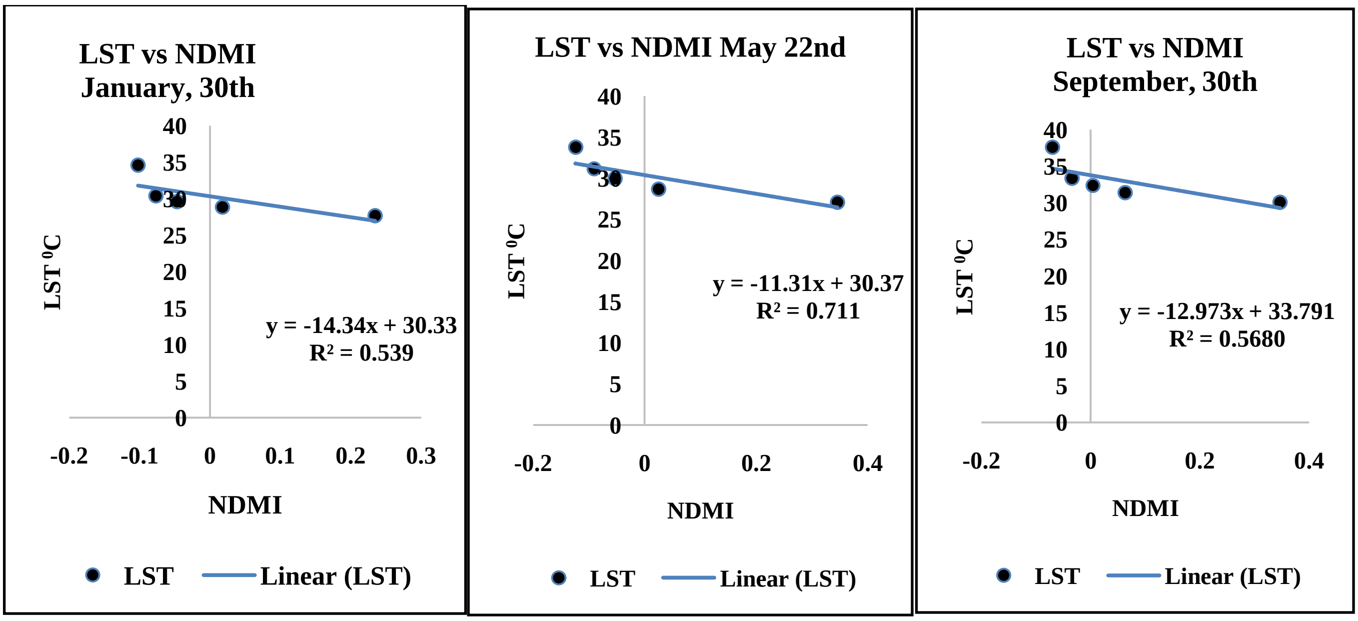

Fig. 9 Correlations between LST and NDMI

I. NDBI and NDMI Correlation

The outcome of the NDBI and NDMI correlation analysis Fig. 10 indicate a negative relationship with R^2 = 0.4831, 0.6809 and 0.5 respectively. Greater Percentage of built-up area is being sealed with the impervious materials with few or scattered trees that give rise to low vegetation moisture.

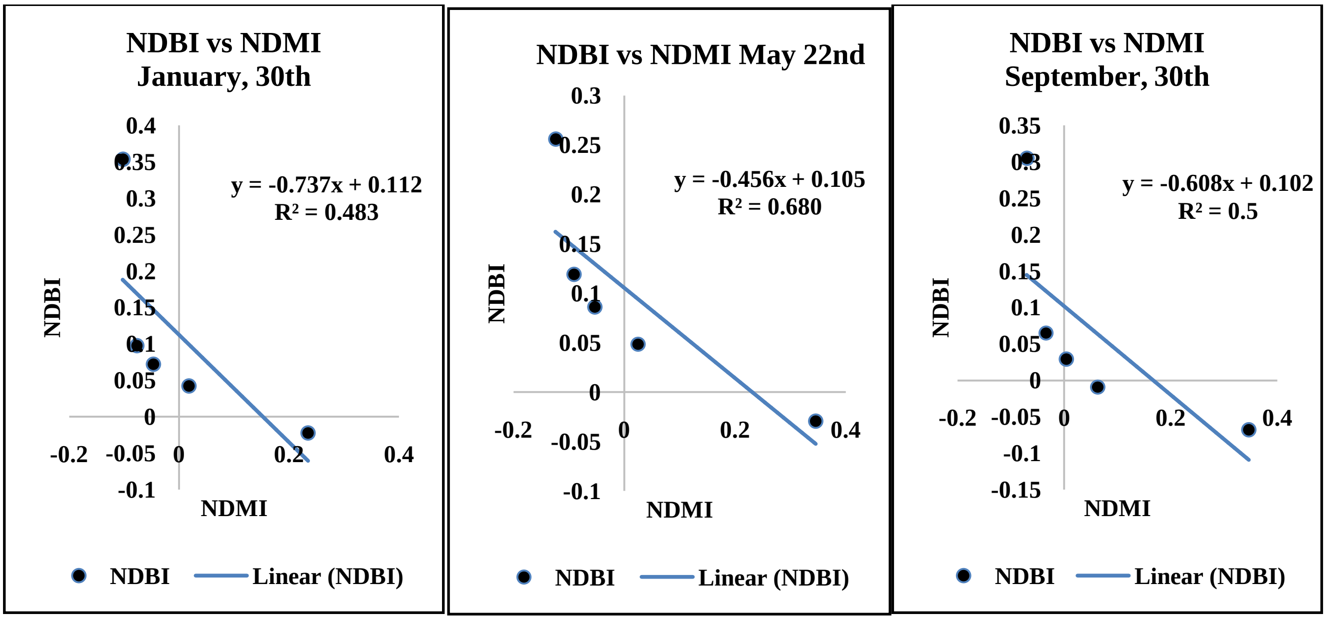

Fig. 10 Correlations between NDBI and NDMI

Conclusion

This study used Landsat 8 and computed LST, NDBI, NDVI and NDMI of Gombe metropolis at three different periods (January 30th, May 22nd, and September 30th in 2019). It was observed that surface temperature of Gombe metropolis is influenced by season and landuse/landcover. Minimum LST was observed in the built-up areas especially part of Tudun Wada, Arawa, Tumfure, Hammadu-kafi, and New Liji, the values are 22.59^{0}C (January 30th), 26.44^{0}C (May 22nd) and 25.20^{0}C (September 30th). The maximum surface temperature was found on rocks and bare surfaces the values are from 34.64^{0}C, 33.95^{0}C and 37.68^{0}C respectively. Maximum NDVI values observed was 0.3198, 0.5214 and 0.5225 respectively and were concentrated on the vegetated areas. The minimum NDVI values -0.0400, -0.0717 and -0.2834 respectively are found in the built-up area of the metropolis. The LST and NDVI correlation reveals a strong negative relation in three periods of study with R^2 = 0.5922, 0.7487 and 0.6017 respectively. The maximum NDBI observed in each period was 0.3539, 0.2561 and 0.3050 respectively and were concentrated on rock surfaces. The minimum NDBI values -0.2344, -0.3457, and -0.3466 respectively were concentrated in vegetated areas. The LST and NDBI correlation analysis shows a strong positive relationship with R^2 = 0.9935, 0.9863 and 0.9923 respectively. Strong negative correlation was observed between NDBI and NDVI with the R^2 = 0.5466, 0.7175 and 0.5368 respectively.

The maximum NDMI values observed was 0.2344, 0.3457 and 0.3466 respectively and were concentrated in the vegetated areas. The minimum NDMI values observed was -0.3539, -0.2561 and -0.3050 respectively and were concentrated on the rock and bare surfaces. The correlation analysis between LST and NDMI reveals a negative relationship with R^2= 0.5399, 0.7115 and 0.5680. Negative correlation was also observed between NDBI and NDMI with R^2 = 0.4831, 0.6809 and 0.5 respectively.

References

[1] Abdulkadir I. SathishKumar J. “Remote Sensing For Monitoring Land Degradation & Sustainable Cities -

[2] A Case Study of Gombe State, Nigeria, M.Tech dissertation, Civil Engineering Department, SRM Institute of Science & Technology, India. June (2020)

[3] Bastiaanssen, W. G. M., Menenti, M., Feddes, R. A., & Holtslag, A.A.M., "A remote sensing surface energy balance algorithm for land (SEBAL) Formulation" Journal of Hydrology, Vol. 212, pp.198–212, (1998)

[4] Su, Z., "The Surface Energy Balance System (SEBS) for estimation of turbulent heat fluxes". Hydrology and Earth System Sciences, Vol.6, pp.85–100, (2002)

[5] Arnfield, A. J., "Two decades of urban climate research: a review of turbulence, exchanges of energy and water, and the urban heat island". International Journal of Climatology, Vol. 23, 1–26, (2003)

[6] Voogt, J. A., & Oke, T. R., "Thermal remote sensing of urban climates" Remote Sensing of Environment, Vol.86, pp.370–384, (2003)

[7] Weng Q, Lu D, Schubring J. "Estimation of land surface temperature-vegetation abundance relationship for urban heat island studies" Remote sensing of Environment, Vol.89, pp.467-483, (2004)

[8] Chen X-L, H-M Zhao, P-X Li, and Z-Y Yin "Remote sensing image-based analysis of the relationship between urban heat island and land use/cover changes" Remote Sens Rev. Vol. 104, No. 2: pp.133-146, (2006)

[9] Kalma, J. D., McVicar, T. R., &McCabe, M. F., "Estimating land surface evaporation: A review of methods using remotely sensed surface temperature data. Surveys in Geophysics, Vol. 29, pp.421–469 (2008)

[10] Weng, Q., "Thermal infrared remote sensing for urban climate and environmental studies: methods, applications, and trends". ISPRS Journal of Photogrammetry and Remote Sensing, Vol.64, pp.335–344, (2009)

[11] Rafiq, M., Rashid, I., & Romshoo, S. A., "Estimation and validation of Remotely Sensed Land Surface Temperature in Kashmir Valley", Journal of Himalayan Ecology & Sustainable Development, Vol. 9, (2014),

[12] Jackson, R. D., S. B. Idso, R. J. Reginato, and P. J. Pinter Jr., "Canopy temperature as a crop water stress indicator", Water Resour. Res. Vol. 17, pp.1133–1138, (1981)

[13] Moran, M. S., Clarke, T. R., Inoue, Y., &. Vidal, A., "Estimating crop water deficit using the relation between surface air temperature and spectral vegetation index". Remote Sens. Environ., Vol.49, pp.246–263, (1994)

[14] Kogan, F. N. "Operational space technology for global vegetation assessment", Bulletin of the American Meteorological Society, Vol. 82 pp.1949–1964, (2001)

[15] Anderson, M. C., Norman, J. M., Mecikalski, J. R., Otkin, J.A., & Kustas, W.P., A "Climatological study of evapotranspiration and moisture stress across the continental United States based on thermal remote sensing: Surface moisture climatology". J. Geophys. Res., Vol. 112, No.10, (2007)

[16] Sun Q, Z Wu, and J Tan "The relationship between land surface temperature and land use/land cover in Guangzhou, China". Environmental Earth Science Vol. 65, No.6, pp.1687-1694, (2012).

[17] Tursilowati L., Sumantyo J.T.S, Kuze H, and Adiningsih E.S. "Relationship between Urban Heat Island Phenomenon and Land Use/Land Cover Changes in Jakarta – Indonesia" Journal of Emerging Trends in Engineering and Applied Sciences (JETEAS) Vol.3, No.4, pp.645-653, (2012)

[18] Chen, L., Li, M., Huang, F., & Xu, S., "Relationships of LST to NDBI and NDVI in Wuhan City based on LANDSAT ETM+ Image", in 6th International Congress on Image and Signal, Processing (CISP2013), (2013)

[19] Clinton, N., Gong, P., "MODIS detected surface urban heat islands and sinks: Global locations and controls" Remote Sensing of Environment Vol. 134, pp.294–304, (2013).

[20] Yusuf Y A, B Pradhan, and M O Idrees, "Spatio-temporal Assessment of Urban Heat Island Effects in Kuala Lumpur Metropolitan City Using Landsat Images" J Indian Soc Remote Sens. Vol.42, No.4, pp.829-837, (2014)

[21] Zaeemdar S. Baycan T. "Analysis of Relationship between Urban Heat Island and Land Cover in Istanbul through Landsat 8 OLI", Journal of Earth Science Climate Change 8: 423, doi:10.4172/2157-7617.1000423 (2017)

[22] Bonafoni Stefania and Chaiyapon Keeratikasikorn "Land Surface Temperature and Urban Density": Multiyear Modeling and

Relationship Analysis Using MODIS and Landsat Data. Remote Sens. Vol.10, 1471; doi:10.3390/rs10091471 (2018a),

[23] Rasul, A. "Global Spatial Relationship between Land Use Land Cover and Land Surface Temperature", Preprints (www.preprints.org). Posted: 3 January 2020 doi:10.20944/preprints202001.0023.v1 (2020),

[24] Bonafoni, S., Keeratikasikorn, C.; "Satellite Images and Gaussian Parameterization for an Extensive Analysis of Urban Heat Islands in Thailand" Remote Sens. Vol. 10, No.665, (2018b) [CrossRef]

[25] Liao, W.; Liu, X.; Wang, D.; Sheng, Y. (2017) "The Impact of Energy Consumption on the Surface Urban Heat Island in China's 32 Major Cities" Remote Sens. Vol. 9, No.250. [CrossRef]

[26] Du, H.; Wang, D.; Wang, Y.; Zhao, X.; Qin, F.; Jiang, H.; Cai, Y. "Influences of land cover types, meteorological conditions, anthropogenic heat and urban area on surface urban heat island in the Yangtze River Delta Urban Agglomeration. Sci. Total Environment, Vol.571, (2016). [CrossRef] [PubMed]

[27] Shahmohamadi, P.; Che-Ani, A.I.; Etessam, I.; Maulud, K.N.A.; Tawil, N.M. "Healthy Environment: The Need to Mitigate Urban Heat Island Effects on Human Health". Procedia Eng. Vol. 20, pp. 61–70, (2011). [CrossRef]

[28] Keeratikasikorn, C.; Bonafoni, S. "Urban Heat Island Analysis over the Land Use Zoning Plan of Bangkok by Means of Landsat 8 Imagery". Remote Sens. Vol. 10, No.440, (2018). [CrossRef]

[29] Kalnay, E., Cai, M., "Impact of urbanization and land-use change on climate" *Nature*, Vol.423, No.528 (2003).

[30] Xian G, Crane M "An analysis of urban thermal characteristics and associated land cover in Tampa Bay and Las Vegas using Landsat satellite data". Remote Sensing of Environment, Vol.104, pp.147-156 (2006),

[31] Zhao C, Fu G, Liu X, Fu F., "Urban planning indicators, morphology and climate indicators: A case study for a north-south transect of Beijing, China". Building and Environment Vol.46, pp.1174-1183, (2011)

[32] Connors J. P, Galletti C. S., Chow W. T., "Landscape configuration and urban heat island effects: assessing the relationship between landscape characteristics and land surface temperature in Phoenix, Arizona". Landscape Ecology Vol. 28, pp.271-283, (2013)

[33] Trenberth K.E., "Climatology rural land-use change and climate". Nature Vol.427, No.213, (2004).

[34] Rasul, A.O., (2016), "Remote sensing of surface urban cool and heat island dynamics in Erbil, Iraq, between 1992 and 2013" (Ph.D.). University of Leicester

[35] Rasul, A., Balzter, H., Smith, C., "Spatial variation of the daytime Surface Urban Cool Island during the dry season in Erbil, Iraqi Kurdistan, from Landsat 8" Urban climate Vol. 14, pp.176–186, (2015)

[36] Suzana Binti Abu Bakar, Biswajeet Pradhan, Usman Salihu Lay & Saleh Abdullahi Spatial assessment of land surface temperature and land use/land cover in Langkawi Island. 8th IGRSM International Conference and Exhibition on Remote Sensing & GIS (IGRSM 2016) IOP Publishing IOP Conf. Series: Earth and Environmental Science 37 (2016) 012064 doi:10.1088/1755-1315/37/1/012064 (2016).

[37] Ma, Q., Wu, J., & He, C. "A hierarchical analysis of the relationship between urban impervious surfaces and land surface temperatures: Spatial scale dependence, temporal variations, and bioclimatic modulation". Landscape Ecology, Vol.31, pp.1139–1153, (2016)

[38] Rajeshwari A and N Mani "Estimation of Land Surface Temperature of Dindigul District using Landsat 8 Data" Int J Res Eng Tech. Vol. 3, No. 5, pp.122-126, (2014),

[39] Rasul A, Balzter H, Smith C. "Applying a normalized ratio scale technique to assess influence of urban expansion on land surface temperature of the semi-arid city of Erbil", International journal of Remote Sensing 38, 3960-3980, (2017)

[40] Mathew, A., Sreekumar, S., Khandelwal, S., Kaul, N., & Kumar, R. "Prediction of surface

temperatures for the assessment of urban heat island effect over Ahmedabad city using linear time series model” Energy and Buildings, Vol. 128, pp.605–616, (2016)

[41] Mushore, T.D., Mutanga, O., Odindi, J., & Dube, T. “Assessing the potential of integrated Landsat 8 thermal bands, with the traditional reflective bands and derived vegetation indices in classifying urban landscapes”. Geocarto International, pp.1–14 doi:10.1080/10106049.2016.1188168 (2016)

[42] Nie, Q., Man, W., Li, Z., & Huang, Y. “Spatiotemporal impact of urban impervious surface on land surface temperature in Shanghai, China”. Canadian Journal of Remote Sensing, Vol.42, No.6, pp. 680–689, (2016).

[43] Raja D. R. “Spatial Analysis of Land Surface Temperature in Dhaka Metropolitan Area” J Bangladesh Institut Plann ISSN 2075: p. 9363, (2012).

[44] Malik M.S., Shukla J.P. & Mishra S., “Relationship of LST, NDBI and NDVI using Landsat-8 data in Kandaihimmat Watershed, Hoshangabad, India. Indian Journal of Geo Marine Sciences Vol. 48, No.1, pp. 25-31, (2019)

[45] Deilami, K., & Kamruzzaman, M. “Modelling the urban heat island effect of smart growth policy scenarios in Brisbane” Land Use Policy, Vol. 64, pp.38–55, (2017)

[46] Estoque, R.C., Murayama, Y., & Myint, S.W. “Effects of landscape composition and pattern on land surface temperature: An urban heat island study in the megacities of Southeast Asia”. Science of the Total Environment, Vol. 577, pp.349–359, (2017)

[47] Igun Eghosa “Analysis and Sustainable Management of Urban Growth’s Impact on Land Surface Temperature in Lagos, Nigeria” Journal of Remote Sensing & GIS Vol. 6, No. 4, DOI: 10.4172/2469-4134.1000212 (2017)

[48] Liang, S., Shi, P., “Analysis of the relationship between urban heat island and vegetation cover through Landsat ETM+: A case study of Shenyang,” Joint Urban Remote Sensing Event. IEEE, pp. 1–5, (2009)

[49] Sumida, A., Watanabe, T., Miyaura, T., “Interannual variability of leaf area index of an evergreen conifer stand was affected by carry-over effects from recent climate conditions”. Scientific Reports 8, 13590, (2018)

[50] Zhang, Z., Ji, M., Shu, J., Deng, Z., Wu, Y., “Surface urban heat island in Shanghai, China: Examining the relationship between land surface temperature and impervious surface fractions derived from Landsat ETM+ imagery”. Int. Arch. Photogramme. Remote Sens. Spat. Inf. Sci, Vol.37, pp.601–606, (2008),

[51] NASA Landsat 8 (L8) data user’s handbook version 5, Last access 21 /2/2021 Available at https://www.usgs.gov/core-science-systems/nli/landsat/landsat-8-data-users-handbook (2019)

[52] Zha, Y, Gao, j. Ni S. Use of Normalized Difference Built-up Index in an automatic mapping Urban area from TM Imagery, International Journal of Remote Sensing, 24, 583-594 (2003)

[53] Aliyu D. "A comparative Study of Soil Fertility Status under Different Agricultural Practice in Gombe Local Government Area" An unpublished B.Sc. Dissertation, Geography Department Bayero University Kano, Nigeria (2002)

[54] National population commission Gombe office, NPC: Census Results. (2007)

[55] Balzerek Heiko "Applicability of IKONOS-satellite scenes: Monitoring, classification and Evaluation of urbanization processes in Africa – Case study of Gombe/Nigeria", (accessed on 9/01/2020) http://citeseerx.ist.psu.edu/viewdoc/download?doi=10.1.1.599.5910&rep=rep1&type=pdf (2001b)